Measuring 2.4 GHz Helix Antennas

It's not very difficult to design and make a helix antenna for a specific frequency and gain. It's more difficult for the serious experimenter to make precise measurements of the finished antenna.

By Paolo Antoniazzi, IW2ACD, and Marco Arecco, IK2WAQ

In 1946, John D. Kraus invented the helical-beam antenna (or axial-mode helix).[1] Commencing with Kraus's correct hypothesis that travelling-wave structures then used in electromagnetic devices would make efficient antennas, the helix antenna has proven to be the radiator of choice for many radio astronomy and space-science applications.

The helical antenna has been carried to the Moon and Mars, and the Navstar GPS satellites use arrays of axial-mode helices. At the end of 1990s, a new interest in helix antennas was born, thanks to the AMSAT Phase 3D program (the well-known AO40 satellite with S-band down links.[2, 3] It's not very difficult to design and make a specific helix for some frequency and gain. It's more difficult for the serious experimenter to make precise measurements of the finished antenna.

Network analyzers, today standard in telecom laboratories, are inaccessible to many amateur experimenters because of budget limits. We have analyzed shortly the possible use of directional couplers, but they are unsuitable because of the very high bandwidth and directivity required for precise microwave measurements. Directivity is the measure of how well the coupler isolates two opposite-travelling (forward and reverse) signals. When measuring reflection coefficient (return loss) of a device under test, directivity is a crucial parameter[4, 5] in the uncertainty of the results. For example, with a coupler directivity of 35 dB and a measured return loss of 30 dB (SWR < 1.07), the measurement error can be between –4 to +7 dB!

To use directional couplers, we need also some form of vector voltmeter (both magnitude and phase angle of the reflection coefficient) so that we can transfer the measured values to a Smith Chart for impedance analysis. At this point, we decided to design and construct a modern version of an instrument famous from early in microwave history: the slotted line.

The measurement of radiation diagrams to obtain helix directivity data

[1]Notes appear on page 22.

Via Roma 18
20050 Sulbiate MI, Italy
paolo.antoniazzi@tin.it

Via Luigi Einaudi 6
20093 Cologno Monzese, Italy
ik2waq@libero.it

is a more conventional task with helices. In effect, the big errors related to direct-reflected wave encountered in Yagi tests[6] are not a problem with circular propagation, because the sense of the reflected wave is reversed. If the receiving antenna is of opposite sense (or the signal received via a reflective path) a signal loss of 20 dB or more results from the cross polarization.

A plane electromagnetic wave is linearly polarized when the electric field lies wholly in one plane containing the direction of propagation. The polarization is vertical when that plane is perpendicular, horizontal when it is parallel to the Earth's surface. A plane electromagnetic wave is circular polarized when the extremity of the electric vector describes a circle in a plane perpendicular to the direction of propagation, making one complete revolution in one period of the wave.

The polarization sense used by the Institute of Electrical and Electronic Engineers (IEEE) is a defacto standard: When viewing the antenna from the feed-point end, a clockwise wind results in right-hand circular polarization (RHCP), and a counterclockwise wind results in left-hand circular polarization (LHCP). When two stations use helical antennas over a nonreflective path, both must use antennas with the same polarization sense. The sense of the helix must be reversed also when feeding a parabolic dish reflector.

The Slotted Line Project

Some types of slotted lines are today available on the surplus market, for example the HP805A and 805C and General Radio type 874-B, but they are expensive. In the seventies, Hewlett Packard also built the 805C, a professional "slotted line" employing two parallel plates (slab line) instead of the normal coaxial line. The equipment, with 40-cm probe travel length, has been realized to work in the frequency range of 0.5 to 4.0 GHz.

A slotted line is essentially a precision 50-Ω, low-attenuation, low-SWR coaxial line intended for precise measurement. For those interested in the project including mechanical realization, the notes in the sidebar "the Slotted Line" are intended as a short tutorial. Our version of slotted line (Fig 1) was realized starting from a 30-cm-long brass square bar, drilled with a precision 14.00-mm hole. Two high-quality Amphenol N female connectors are fixed at the two ends of the bar. The center pins of two panel connectors support the internal precision rod (diameter = 6.08 mm for an exact 50-Ω line) made in gold-plated copper. One side of the rod is soldered, the other side is connected via a homemade spring contact. This point is very critical to obtain the targeted very low SWR. Table 1 shows the maximum permissible mechanical errors. A probe, mounted on a carriage (as shown in Fig 2), which is movable in a narrow (3 mm) slot cut longitudinally along the outer conductor, extends into the line to sample the RF field.

In the past the probe was a diode. Today the best solution is a very small loop connected via a short cable and a 6-dB attenuator to a broadband 20-dB preamplifier. The input attenuator is needed to avoid the risk of amplifier oscillations. For some tests we also used a Drake 2880 converter followed by a Boonton RF millivoltmeter, model 92B.

Possible Sources of Errors with Slotted Lines

The primary function of a slotted line is to provide a method of detecting a standing wave pattern along a transmission line. Thus, to faithfully reproduce this pattern, the critical parameters are the residual SWR and the possible irregularities. The commercial slotted lines, manufactured to work at these frequencies, have guaranteed SWR ≤ 1.04 and 0.2 dB of irregularities. A line with a perfect 50-Ω characteristic impedance is related to the fact that both SWR and impedance measurement accuracy are strictly linked to this value.

For this reason, the manufacturing phase requires attention to all possible errors caused by dimensional tolerances. They have been analyzed individually even if, at the end, their effects may overlap.

The first one is related to the ratio between the inner diameter of outer conductor D and the outer diameter of the inner conductor d that must be exactly 2.30 to have a perfect 50-Ω characteristic impedance as described by the following expression [7]:

$$Z_0 = 60 \ln\left(\frac{D}{d}\right) \qquad \text{(Eq 1)}$$

In Table 1, the slotted-line SWR changes versus mechanical data (tolerances) are shown. For instance if we consider D = 14.00 mm and SWR = 1.02, the d tolerance will be about ±0.10 mm. Remember that a value of SWR = 1.02 is equivalent to a resistive characteristic impedance change of ±1 Ω or ±0.5%.

Another error that prevents obtain-

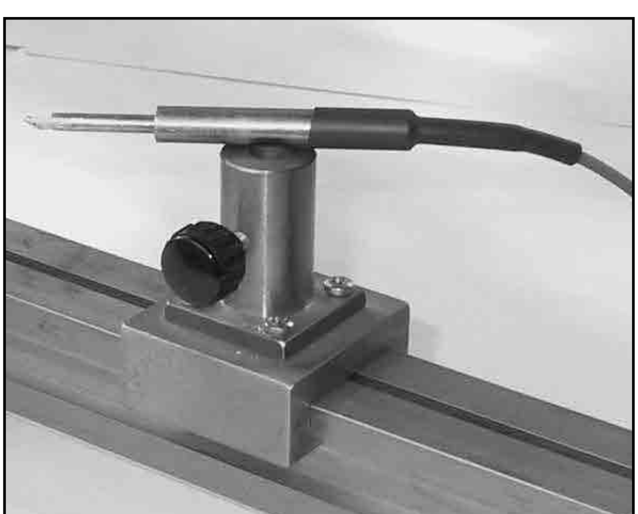

Fig 1—The complete homebrew slotted line.

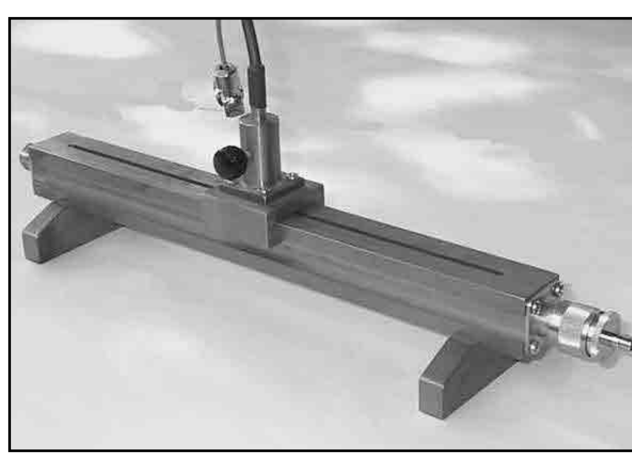

Fig 2—Carriage and probe of the slotted line.

ing a perfect 50-Ω characteristic line impedance is related to the placement of the inner conductor exactly at the center of the outer one. In the ideal case, the two symmetry axes must coincide. In the following equation is reported the relation between the eccentricity *c* and the characteristic impedance of the line (from Note 7):

$$Z_0 = 60 \cosh^{-1}\left(\frac{\frac{D}{d}+\frac{d}{D}-\frac{4c^2}{d\,D}}{2}\right) \quad \text{(Eq 2)}$$

The change of characteristic impedance versus the eccentricity *c* (that is the distance between the center lines of the inner and the outer conductors) is reported in Table 1. The described values are relative to our case (D = 14 mm and d = 6.08 mm). If we consider SWR = 1.02; the maximum eccentricity allowed is 0.80 mm.

A third source of error can be the discontinuity created by the longitudinal slot on the outer conductor (to detect the field within the slotted line via a very small loop probe). Nevertheless its impact is negligible as can be seen looking at the following equation (from Note 7):

$$\Delta Z = 0.03\theta^2 \quad \text{(Eq 3)}$$

where:

ΔZ = characteristic impedance increase compared with a 50-Ω coaxial line.

θ = angular opening of the slot (in radians).

Cables and Coaxial Adapters: A Very Critical Point

One of the critical points in very low SWR measurements is the extremely high quality required of the cables and adapters.[8] The time and money spent on high-quality cables can be wasted if there are large impedance mismatches within the connectors, at the connector-cable interface and with the adapters (typically N to SMA, for the device in test). David Slack of Times Microwave Systems writes:

> "…a microwave cable assembly is not just a wire. It is a passive, TEM mode, microwave component and an integral part of a system…."

Assuming a high-quality cable is used, the predominant contributor to the SWR of a cable assembly (on a 10-50 cm short assembly) is the connector. Improperly compensated geometry changes in the connector interface will exhibit very poor SWR characteristics.

In previous eras, this design was considered a "black art," and trial and error was a key component of high-performance design. Today, the computer simulation of discontinuities in connectors is an art, and the practical results are visible when the SWR performance of a very good cable assembly (N-male connectors) as that of the Times Microwave Systems is shown (Note 8). Only N and SMA connectors are used in our tests.

The characteristic impedance of the slotted line also may be affected by SWR induced by incorrect characteristic impedances of parts of the line, particularly at the transition between the inner conductor and the N-type panel connector lead that have different dimensions.

The following equation gives the SWR of the whole line when a small part of it ($L < 0.1\,\lambda$) does not match the characteristic impedance of the line under test:[9]

$$SWR = 1 + 2\pi\left(SWR_1 - \frac{1}{SWR_1}\right)\frac{L}{\lambda} \quad \text{(Eq 4)}$$

where:

SWR_1 = SWR of the mismatched part of the line: either Z_1 / Z_0 or Z_0 / Z_1 so that $SWR_1 \geq 1$.

Z_1 = characteristic impedance of the mismatched part of the line (ohms)

L = length of the mismatched part of the line (mm)

Z_0 = characteristic impedance of the main line (ohms)

λ = wavelength in the line (mm)

To clarify use of the above equation, let's perform an example.

If Z_0 = 50 Ω; Z_1 = 35 Ω; L = 1 mm; λ = 125 mm, the total SWR increases to 1.04:1 with a discontinuity of the characteristic impedance of only 1 mm. Analyzing the possible errors during the slotted-line manufacturing phase, it is considered a low SWR value because its worst case can increase rapidly as reported below.

Several components are used to connect the slotted line to the load: adapters, connectors and cables. These components can introduce very important impedance mismatches, and the worst-case standing wave ratio can increase rapidly, as can be seen by applying the following simple expression considering four mismatches:

$$\rho_{\text{total}} \quad \rho_1\rho_2\rho_3\rho_4 \quad \text{(Eq 5)}$$

A numerical example will clarify this quick SWR increase. For instance, an SWR = 1.02—that is very small—can become 1.08 considering four similar mismatch sources.

First Measurements of SWR and Impedance

The use of a slotted line is becoming a lost art; but to learn about it is not so difficult. The first suggested measurement with a new slotted line is the SWR of the system terminated on a very good commercial termination. Our first results with an old HP termination model 909A (N-male connector) were not the best, but the 909A is guaranteed no better than SWR = 1.04. The results are better using the famous Minicircuits[10] type Anne-50 with SMA-male connector (SWR = 1.03 at 3 GHz) and a good Amphenol N-male/SMA-female adapter. The

Table1

Maximum permissible mechanical errors

SWR	*1.00*	*1.01*	*1.02*	*1.05*	*1.10*
RL (dB)	*∞*	*46*	*40*	*32*	*26*
|ρ|	*0*	*0.005*	*0.010*	*0.024*	*0.048*
D/d	2.30	2.28	2.26	2.21	2.13
		2.32	2. 34	2.40	2.50
D (mm)	14.00	—	—	—	—
d (mm)	6.08	–0.05	–0.10	–0.24	–0.48
		+0.06	+0.11	+0.25	+0.51
D (mm)	14.00	–0.13	–0.25	–0.55	–1.04
		+0.11	+0.24	+0.60	+1.21
D (mm)	6.08	—	—	—	—
c(mm)	0	0.57	0.80	1.24	1.69

measured values on our slotted line are shown in Fig 3. For almost all tests, we used a signal generator from 2.2 to 2.6 GHz composed of a JTOS-3000 VCO followed by an MNA-6 amplifier (3´3 mm package).

Another important point: Make sure to use the correct RF signal levels during measurements. The input level from the oscillator is very high (+10 dBm), but some attenuation must be included for stability (the wide-band amplifiers oscillate very easy with loads that are not exactly 50 Ω). Using the Boonton RF Millivoltmeter (model 92B) as a detector, we have also a sensitivity attenuation of about 10 dB at 2.4 GHz (referred to the maximum suggested operating frequency of about 1.2 GHz) and consequently the level sampled by the probe is very low (typically 0.3 to 3 mV). In future measurements, we will use a 2.2 to 2.6 GHz heterodyne system composed of a harmonic mixer and a 1.05 GHz fixed-frequency local oscillator. The IF will be in the range 100-500 MHz, limited by a 550 MHz low-pass filter. This solution is free from oscillation risks, and the gain is obtained with a simple wide-band amplifier followed by the RF millivoltmeter. In effect, it's very important to minimize the coupling of the probe to the line to obtain reliable results.

Simulation and Measurement of Helices

After a short but necessary didactical phase, we will go speedily to the helix antennas. Using *NEC* and particularly the powerful *NEC-WinPro* software[11, 12] as a simulation tool and starting from the important results obtained by the simulation work of D. T. Emerson (Fig 4)[13] we have analyzed two different antennas (Fig 5). One is a simple unit of five turns (gain = 12 dBi) and one is 16.7 turn with 14.5 dBi gain. A more complex antenna named TriHelix, a 18 dB array of 16.7 turn helices feed via three flat

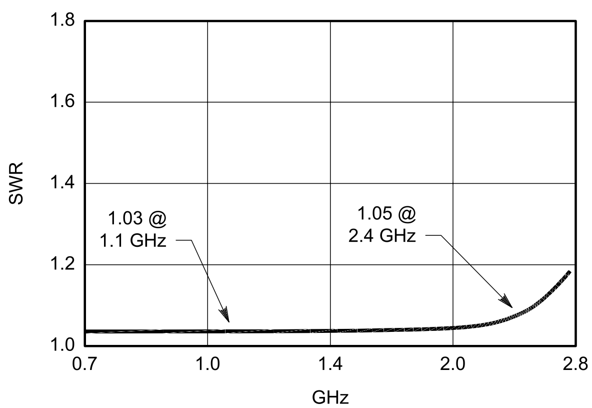

Fig 3—Measured slotted line: a very good SWR from 500 to 2800 MHz.

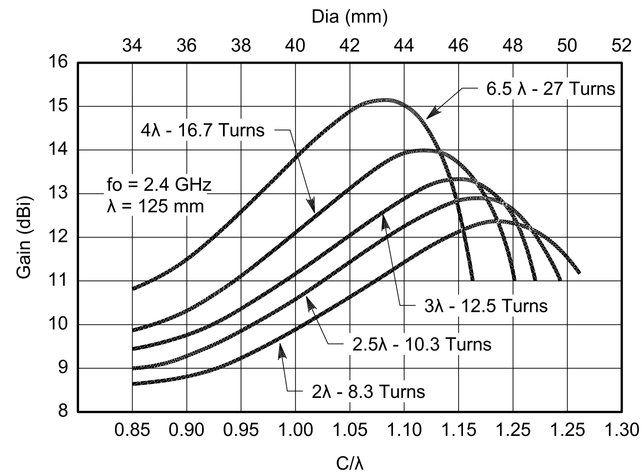

Fig 4—Simulated gain versus helix diameter and C/λ at 2.4 GHz.

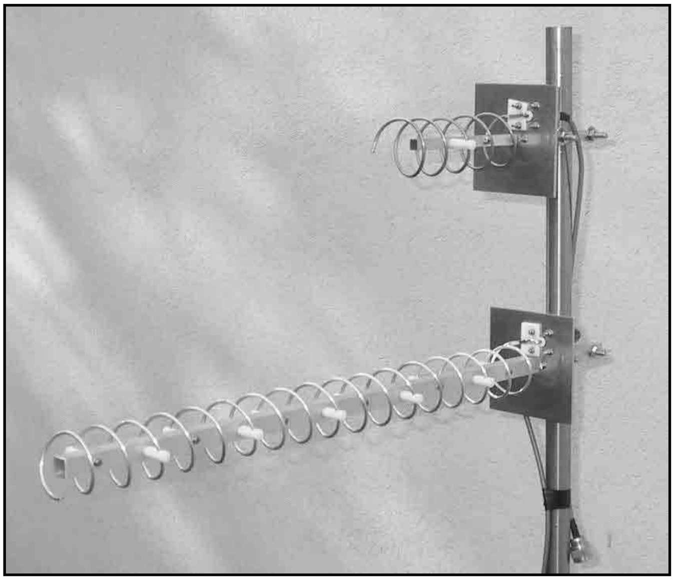

Fig 5—Five turn and 16.7 turn helices in test.

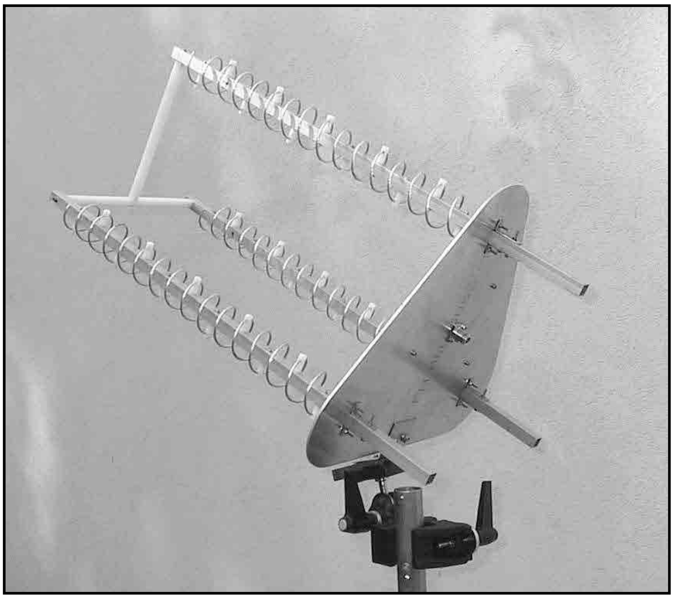

Fig 6—Experimental trihelix antenna.

130-Ω air-dielectric lines (see Fig 6), is in an experimental phase.

The *NEC-Win Pro* software allows simple wire modeling of the helix antenna using the "GH" card (the name card came from *Fortran*). This card avoids the need to calculate the coordinates of each segment using a spreadsheet software (such as *Lotus 1-2-3*, *Excel* and so on) and transfer them to *NEC-Win Pro* as text with risk of errors. To describe a helix however complex, the "GH" card needs only eight parameters:

Number of segments.
Spacing between turns (0.24 λ or 30 mm at 2.4 GHz for our helices).
Helix radii in two perpendicular directions, at both the beginning and end of the winding (this feature allows us to simulate both elliptic and conical helices).
Total helix length.
Wire diameter.

To simulate the helix, we decided to use ten segments per turn as a good trade-off between the *NEC-Win Pro* rules and the need for a better description of the circular shape of the antenna. To be unidirectional, a helix needs a suitable ground plane near the feed point. It can be made with *NEC-Win Pro* using a square grid plate (125×125 mm, λ at 2.4 GHz). This kind of structure needs a number of segments given by the following general equation:

$$N \quad 2n(n+1) \qquad \text{(Eq 6)}$$

where n is the grid factor (the number of parts in which the plate is divided by the wires that compose it).

In our case, with the purpose of minimizing the current within the screen, we decided to use n = 20 (0.05 λ pitch between wires), and so the plate is composed of no less than 840 segments. With the same purpose of minimizing the current in the screen, a 6-mm-long stub has been added between the helix and the grid plate. This requirement for a large number of screen segments prevents use of a grid plate when the total number of segments exceeds the 2000 available with the *NEC-Win Pro* software. In this last case, it is possible to simulate it by using a perfect ground and orienting the helix symmetry axis vertically.

We tried to simulate the helices both with the grid screen and a perfect ground and the differences detected in power gain, radiation angle and feed impedance are not significant. The only big difference is the loss of the radiation pattern at the back of the antenna when using the perfect ground.

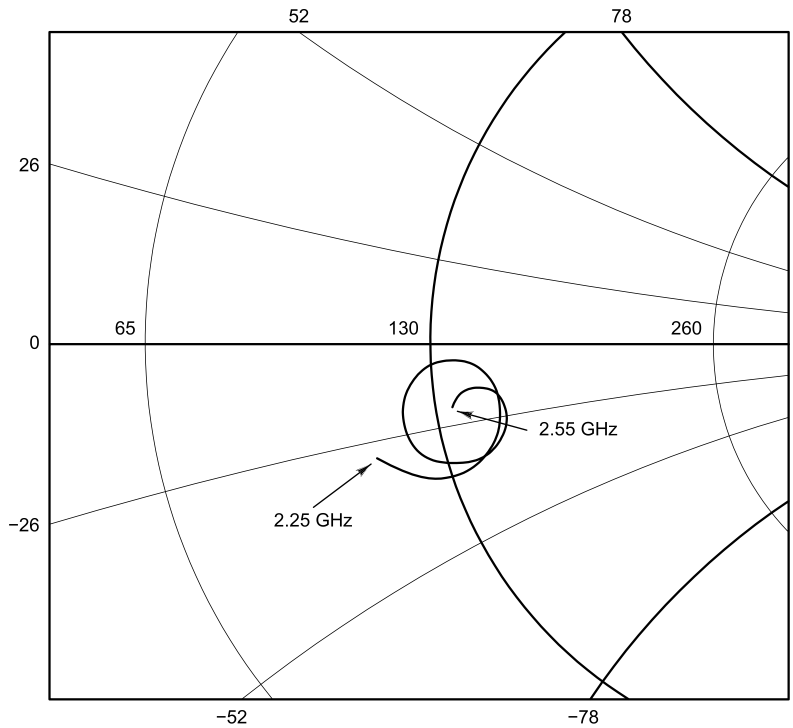

Fig 7—Simulated input impedance of the 16.7 turn helix.

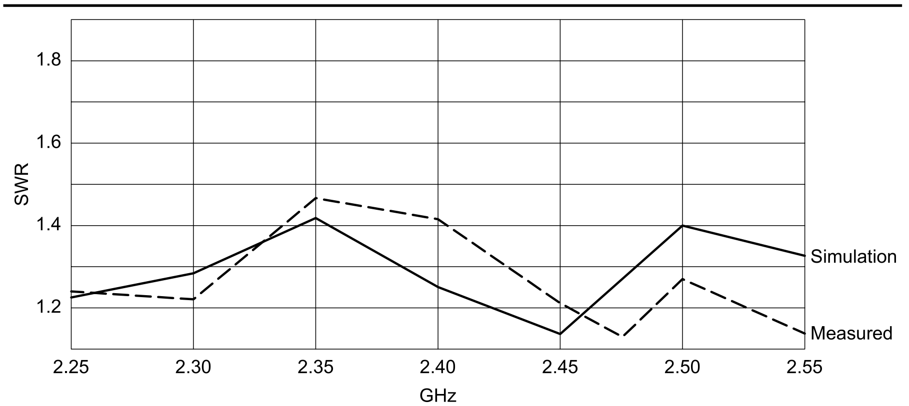

Fig 8—First approach to the SWR versus frequency of a 16.7 turn helix.

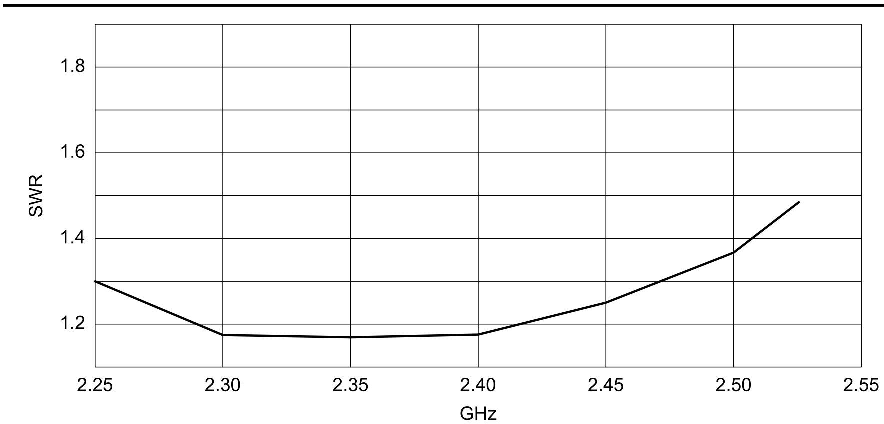

Fig 9—Finally tuned 16.7 turn helix: measured SWR versus frequency.

Also, the screen can be simulated easier with the "GM" card that allows the repeating and the moving of the segments with only few statements, with respect to the full description of the segments.

The files of the 5 and 16.7 turn helices will be supplied to interested experimenters by e-mail on request.

The simulated values for the input impedance (referred to 130 Ω) of the 16.7 turn helix are shown in Fig 7. The simulation of SWR values and the first measured values from 2.25 to 2.55 GHz are visible in Fig 8. In Fig 9, the measured values for the finally tuned helix are shown. The matching between the 130-Ω nominal input impedance of the single helix and 50 Ω is obtained via a λ/4 transformer (Teflon support with h = 2.5 mm and line with W = 3 mm, Z = 81 Ω). The transformer layout is shown in Fig 10 (calculated using a good HP tool, *AppCad*.[14] See also the photo of Fig 11 where the real Teflon impedance adapter is shown at the beginning of the five-turn helix. The first measurements on the TriHelix antenna give a SWR = 1.3-1.4 at 2.4 GHz ±100 MHz. With the multiple-helix arrays the mutual impedance of adjacent helices is to be considered, but when separated by a wavelength or more, as is typical in helix arrays, the mutual impedance is only a few percent or less of the helix self impedance (130-140 Ω). Thus in designing the feed corrections for a helix array, the effect of the mutual impedance can often be neglected (see Note 1) without significant consequences.

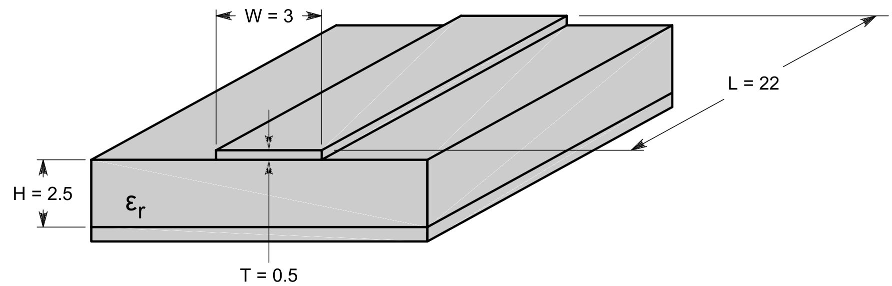

Fig 10—Layout of the λ/4 Teflon transformer calculated using HP-*AppCAD*. This is a λ/4 transformer from 130 Ω to 50 Ω. The transformer is realized using a Teflon plate (22×30 mm) and a copper strip with *W* = 3 mm and *T* = 0.5 mm at the beginning of the helix.

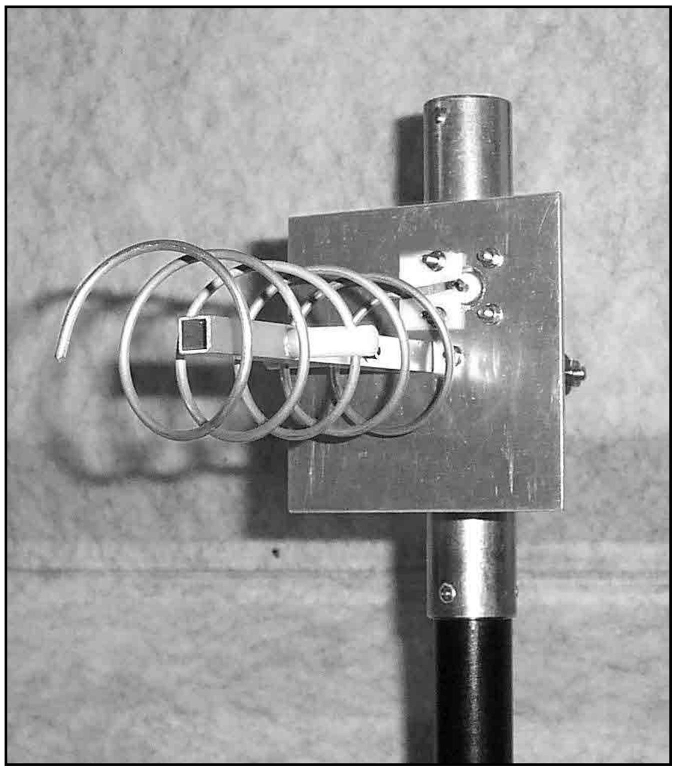

Fig 11—Five turn helix (see the λ/4 79 Ω Teflon adapter).

Free Space Attenuation

To reduce the measurement errors, the distance between transmitting and receiving antennas must be considered. To determine this distance, you need to measure the signal level with a filtered RF voltmeter having a 30-40 dB dynamic range. Also, the wave reaching the receiving antenna should be as planar as possible.

The first condition can be easy established starting with the received power and calculating the attenuation experienced by the wave in the open space:

$$\alpha \quad 32.4 + 20\log(f) + 20\log(d - G_t - G_r \qquad \text{(Eq 7)}$$

Here, a is the attenuation in decibels, f is the frequency (megahertz), d is the distance (km), G_t is the gain of transmitting antenna (dBi) and G_r is the gain of receiving antenna (dBi) obtained by simulation.

There is also a simple, easy-to-remember method of calculating the

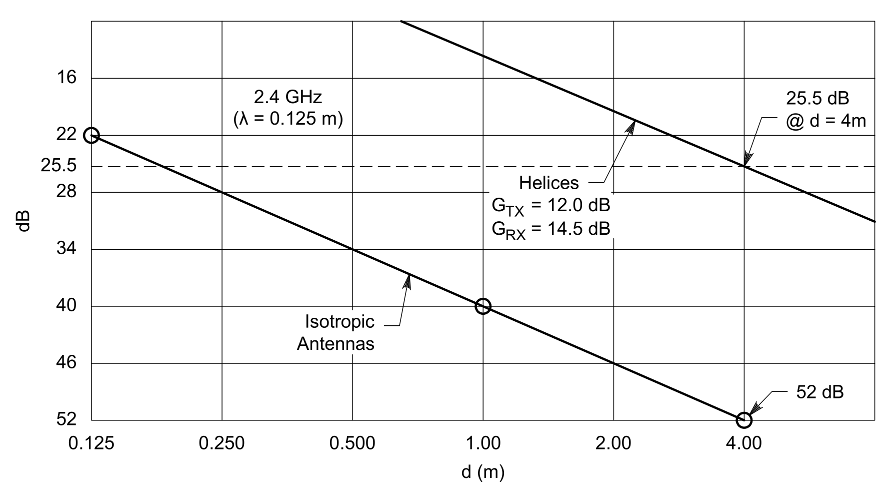

Fig 12—Free-space attenuation at 2400 MHz.

free-space attenuation by considering the distance between the two antennas in terms of wavelengths. When $d = \lambda$, α is always 22 dB between isotropic antennas.

This equates to 12.5 cm at 2400 MHz. The attenuation increases by 6 dB for each doubling of the path distance. This means that the free space attenuation is 22 dB at 0.125 m, 28 dB at 0.25m, 34 dB at 0.5 m, etc (see the diagram of Fig 12). To make the wave reaching the receiving antenna as planar as possible, the capture area of the receiving antenna in square meters and the maximum acceptable phase error are needed:

$$\alpha \quad \frac{G_r \lambda^2}{4\pi} \qquad \text{(Eq 8)}$$

This expression is valid for an antenna with no thermal losses and was certainly useful for our experiments. Assuming that the capture area is circular, the minimum distance in meters between the antennas will be:

$$d >= \frac{n G_r \lambda}{\pi^2} \qquad \text{(Eq 9)}$$

For a maximum phase difference of 22.5°, which is usually enough, $n = 2$. If a phase error of only 5° is required, $n = 9$. In the case where one dimension prevails over the others, the maximum length, instead of the capture diameter, is used. In this case, the minimum distance in meters becomes, (Note 7)[15, 16]:

$$d >= \frac{n L}{\pi^2} \qquad \text{(Eq 10)}$$

where L is the maximum length in meters (50 cm for the 16.7-turn helix).

The site we selected (in the garden) is particularly useful for our measurements and equates d = 4 m = 32 λ at 2400 MHz. For a lot of very useful information on antenna measurements, see also Kraus.[17]

Radiation Diagrams, Efficiency and Gain

In Figs 13 and 14, the radiation diagrams of the 5- and the 16.7- turn helices, obtained via the *NEC-Win Pro* simulation, are shown with gains in dBi. The directivity of an antenna is based entirely on the shape of radiated power pattern and does not consider the minor lobes. In this parameter, the antenna efficiency is not involved.

The gain of an antenna is defined as a ratio of a maximum radiation intensity of the antenna to a maximum

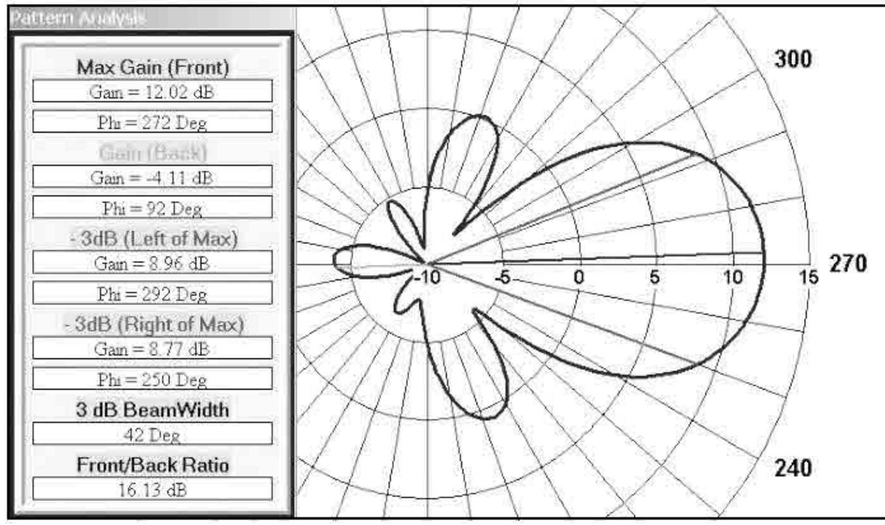

Fig 13—Five turn helix radiation diagrams: simulation with *NEC-Win pro*.

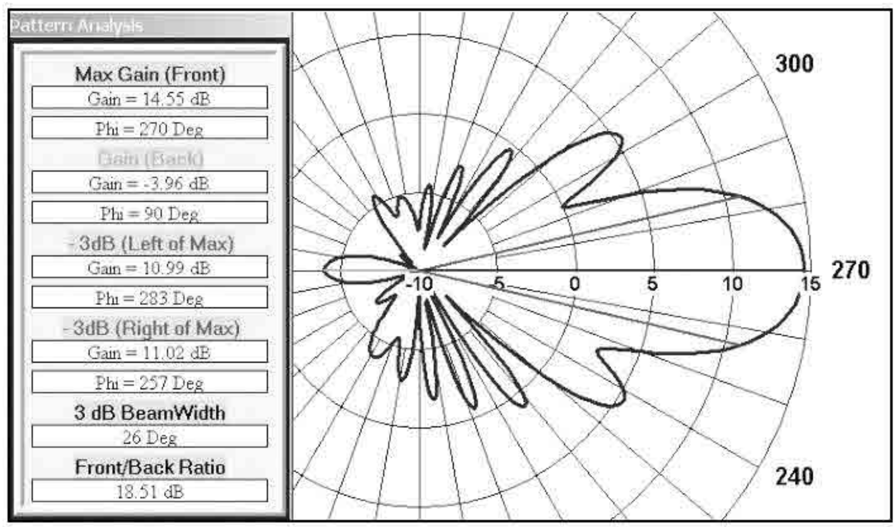

Fig 14—Radiation diagrams for the 16.7 turn helix: simulation with *NEC-Win pro*.

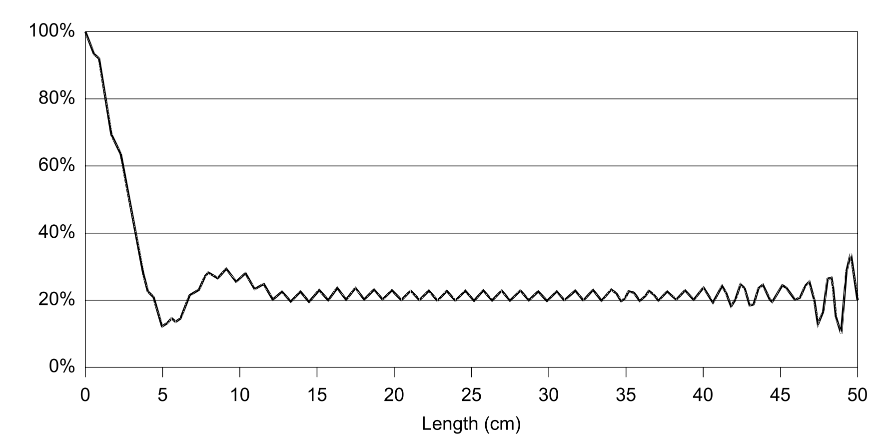

Fig 15—Simulated helix current for a 16.7 turn antenna.

Slotted Line

A "slotted line" is an air-dielectric, low-loss coaxial transmission line (<0.3 dB) having precisely 50 Ω characteristic impedance. It is 30 to 50 cm long, depending on the lowest working frequency, and at the ends it presents two connectors, generally N type, for connection to a RF generator, a load or a line to be measured. Along the outer conductor of the coaxial line is a narrow longitudinal slot, in which is placed a small probe. The penetration of the probe into the line is a tradeoff between the voltage levels to be detected and the need to minimize the perturbation of the line field in which it is immersed. An RF millivoltmeter is used to detect the field existing in the slotted line. It is connected to the probe via a shielded cable. The probe is placed on a sliding carriage that can move along the line. Its position can be read with a resolution of about 0.5 mm by a pointer moving along a suitable ruler fixed to the slotted-line body. The instrument's low-frequency limit is a function of the maximum length on which the carriage probe can travel. When a generator is connected at one end of the slotted line and a load to the other one, we have two possibilities: the load has impedance equal to the characteristic impedance (Z_0) or not. In the first case, we have no reflection from the load and the voltage detected by the probe along the line is flat. If the load impedance differs from Z_0, a standing-wave pattern occurs and moving the probe along the line we will find one or more maxima (loops) and minima (nodes). In this case, the distances between two contiguous maxima (see Fig 16) or minima is one-half wavelength, and so we are able to estimate the frequency of the RF source used to feed the load. We are also able to calculate the SWR using the following equation:

$$SWR = \frac{e_{MAX}}{e_{min}} \quad \text{(Eq 12)}$$

or Return Loss in decibels:

$$RL = 20\log\left(\frac{e_{MAX} + e_{min}}{e_{MAX} - e_{min}}\right) \quad \text{(Eq 13)}$$

where

e_{MAX} = maximum voltage, measured with the probe, along the slotted line (mV).

e_{min} = minimum voltage, contiguous to the previous maximum, measured with the probe (mV).

Moreover, the slotted line gives us the capability to calculate the impedance, both real and imaginary parts, measuring the node displacement when the line is connected to the load and the load is replaced by a short circuit.

The computation of the complex impedance can be performed using the expression of the lossless line:

$$Z = Z_0 \frac{Z_L + jZ_0 \tan(\beta l)}{Z_0 + jZ_L \tan(\beta l)} \quad \text{(Eq 14)}$$

where

β = phase constant: $2\pi / \lambda$, (cm^{-1})

l = node displacement, (cm).*

λ = wavelength, (cm).

The same kind of calculation can be performed more easily with the aid of the Smith chart.

The slotted line can also be used to establish the cable attenuation, repeating the SWR measurement at both the beginning and the end of the line to be tested.

The computation of the attenuation A (in decibels) can be performed using the following equation derived from the one for lossy lines:

$$A = \left[\tanh^{-1}\left(\frac{1}{\rho_1}\right) - \tanh^{-1}\left(\frac{1}{\rho_2}\right)\right] 8.69 \quad \text{(Eq 15)}$$

where

ρ_1 = SWR at the beginning of the line.

ρ_2 = SWR at the end of the line.

*Pay attention that, in the evaluation phase, the maximum displacement allowed is ±λ/4.

radiation intensity of a reference antenna with the same power input—in the gain the antenna efficiency is involved.

The helix antenna power gain (in dBi) can be computed using the following:

$$G = 10\log_{10}\left(\frac{360^2\eta}{\pi\,\theta^2}\right) \approx 10\log_{10}\left(\frac{41{,}253\,\eta}{\theta^2}\right) \quad \text{(Eq 11)}$$

where:

θ = main-lobe radiation angle at half power, in degrees

η = efficiency (< 1)

In Table 2, there are computations of the power gains of the 5- and 16.7-turn helices as functions of the measured radiation angles and efficiency. We can see that increasing the length

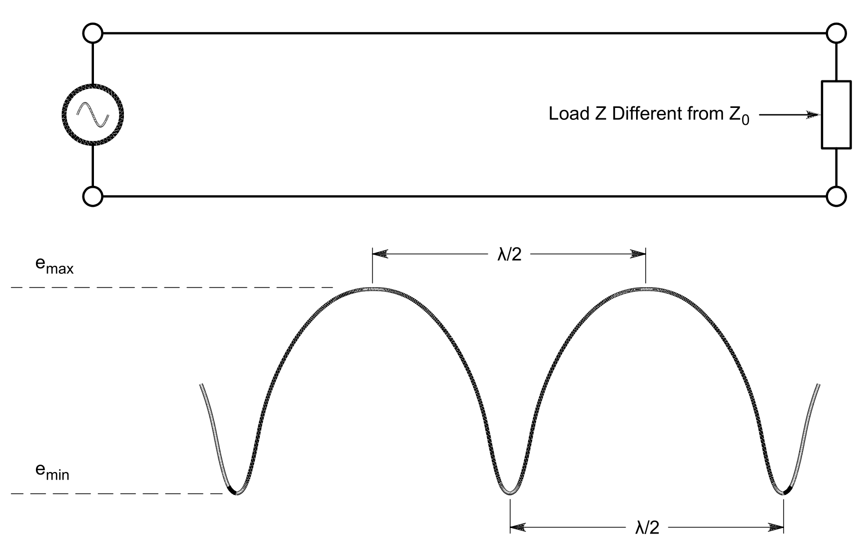

Fig 16—A standing wave on a transmission line terminated by a load impedance different from the line characteristic impedance (50 Ω in our case).

of the helix (from 150 mm to 500 mm) decreases its efficiency. The measured and simulated values of helix gain are shown in Table 3.

The measured radiation lobes (–3 dB) at 2400 MHz agree within about ±1.5 degrees with the calculated values on both the helices. The simulated behavior of the current in the helix versus antenna length is shown in Fig 15. As you can see, the current decayed exponentially near the input end; there was a standing wave over a short distance near the open end, while there was a relatively uniform current amplitude (small SWR) between the ends, which extended over most of the helix.

Notes

[1]J. D. Kraus, *Antennas*, second edition (New York: McGraw-Hill, 1988) "The Helical Antenna," pp 265-339.

[2]"Microwave Radio via AMSAT Oscar AO-40," *RadCom* (Hertfordshire, England: RSGB), Aug 2001.

[3]"A Practical Approach to Operating AO-40," *RadCom*, Nov/Dec 2001.

[4]P. Antoniazzi, "High Directivity RF Coupler," *Electronics World*, Oct 1966, pp 763-765.

[5]"HP-Dual Directional Coupler, Model 778D," technical brochure, 1982.

[6]P. Antoniazzi and M. Arecco, "Measuring Yagis," *Electronics World*, Dec 1998, pp 1002-1006.

[7]*Reference Data for Radio Engineers,* fifth edition, (Indianapolis, Indiana, USA: H. W. Sams & Co, 1989) pp 29-19 to 29-23.

[8]D. Slack, "Microwave and RF Cable Assemblies: the Neglected System Component," *Applied Microwave & Wireless*, Nov/Dec 1997, pp 36-45.

[9]M. W. Dixon (Ed), G3PFR, *Microwave Handbook* Vol 1, (RSGB, 1989) pp 5-22.

[10]**www.minicircuits.com**.

[11]*NEC-Win Pro*, release 1.4, 2002 (Nittany Scientific Inc; **www.nittany-scientific.com**).

[12]W. Walker, W5GFE, "*A Perl/Tk Package for NEC* Based Antenna Design," *QEX*, May/Jun 2001, pp 51-54.

[13]D. T. Emerson, "The Gain of the Axial-Mode Helix Antenna: A Numerical Modeling Study," March 1995, National Radio Observatory, Tucson, Arizona, USA.

[14]*AppCAD*, is a free download from Agilent. For the 14.5 MB download, visit **www.educatorscorner.com/index.cgi?CONTENT_ID=2601** and page down to "RF Cool Links." You can order the application on CD by e-mailing **semiconductorsupport@agilent.com**.

[15]*The ARRL Antenna Book*, 16th edition (Newington, Connecticut, USA: ARRL, 1992).

[16]D. R. J. White, *Electromagnetic Interference and Compatibility*, Vol 2, 1980. Published by Don White Consultants, State Rd 625, PO Box D, Gainesville, VA 22065.

[17]J. D. Kraus, *Antennas*, second edition, (McGraw-Hill, 1988) "Antenna Measurements," pp 805-843.

Paolo Antoniazzi, IW2ACD, is a Technical Information Manager in the TPA-Central Marketing department of STMicroelectronics. He has more than 35 years of experience in RF and audio applications. Paolo is a member of IEEE, RSGB, ARI (Associazione Radioamatori Italiani) and the Audio Engineering Society. He was first licensed in the early 1960s, and in February 2003 obtained a "Ruolo d' Onore ARI" (40 years of ARI membership). His amateur interests include slow CW in the LF band and simulation and tests of antennas from LF loops to VHF-µW.

Marco Areco, IK2WAQ, is a Standard Nonvolatile Memories Product Engineering Team Leader with more than 30 years experience in semiconductor manufacturing. Marco is a member of ARI. He has been licensed 10 years and his amateur interests include LF operations and VHF, UHF, µW antenna simulations and measurements.

Table 2

Helix radiation angles, efficiency and gain

	5.0 Turns, L = 150 mm (degrees)			*16.7 Turns, L = 500 mm (degrees)*		
Efficiency (%)	*41*	*42*	*43*	*24*	*25*	*26*
70	12.3	12.1	11.9	17.0	16.6	16.3
65	12.0	**11.8**	11.6	16.7	16.3	16.0
60	11.7	11.5	11.3	16.3	16.0	15.6
55	11.3	11.1	10.9	16.0	15.6	15.3
50	10.9	10.7	10.5	15.5	15.2	14.8
45	10.4	10.2	10.0	15.1	**14.7**	14.4
40	9.9	9.7	9.5	14.6	14.2	13.9
35	9.3	9.1	8.9	14.0	13.6	13.3
30	8.	8.5	8.3	13.3	13.0	12.6

Table 3

Comparison of simulated and measured helix gain

HELIX	*L (λ)*	*NECWinPro Simulation (dB)*	*Emerson (*) Simulation (dB)*	*Emerson (**) Simplified Formula (dB)*	*Measured Values (dB)*
5.0 turns	1.2	12.0	-	11.6	**12.5**
16.7 turns	4.0	14.5	14.0	14.0	**15.0**

*See Reference 13
**G = 10.25 + 1.22 L –0.00726 L^2

□□